BIOCHEMISTRY
including biophysical chemistry & molecular biology

Article

pubs.acs.org/biochemistry

Mapping the Conformational Stability of Maltose Binding Protein at the Residue Scale Using Nuclear Magnetic Resonance Hydrogen Exchange Experiments

Céline Merstorf,[†] Olek Maciejak,[†,‡] Jérôme Mathé,[†] Manuela Pastoriza-Gallego,[†] Bénédicte Thiebot,[†] Marie-Jeanne Clément,[‡] Juan Pelta,[†] Loïc Auvray,[§] Patrick A. Curmi,*[,‡] and Philippe Savarin*[,‡]

[†]Centre National de la Recherche Scientifique (CNRS) UMR 8587, Université Evry-Val d'Essonne et Cergy Pontoise, Laboratoire d'Analyse et de modélisation pour la Biologie et l'Environnement, Evry 91025, France

[‡]Institut National de la Santé et de la Recherche Médicale (INSERM), UMR 829, Université d'Evry-Val d'Essonne, Laboratoire Structure-Activité des Biomolécules Normales et Pathologiques, Evry 91025, France

[§]Centre National de la Recherche Scientifique (CNRS) UMR 7057, Université Paris Diderot, Matière et Systèmes Complexes, Paris 75205, France

Supporting Information

ABSTRACT: Being able to differentiate local fluctuations from global folding−unfolding dynamics of a protein is of major interest for improving our understanding of structure−function determinants. The maltose binding protein (MBP), a protein that belongs to the maltose transport system, has a structure composed of two globular domains separated by a rigid-body "hinge bending". Here we determined, by using hydrogen exchange (HX) nuclear magnetic resonance experiments, the apparent stabilization free energies of 101 residues of MBP bound to β-cyclodextrin (MBP−βCD) under native conditions. We observed that the last helix of MBP (helix α14) has a lower protection factor than the rest of the protein. Further, HX experiments were performed using guanidine hydrochloride under subdenaturing conditions to discriminate between local fluctuations and global unfolding events and to determine the MBP−βCD energy landscape. The results show that helix α4 and a part of helices α5 and α6 are clearly grouped into a subdenaturing folding unit and represent a partially folded intermediate under native conditions. In addition, we observed that amide protons located in the hinge between the two globular domains share similar ΔG_{gu}^{app} and m values and should unfold simultaneously. These observations provide new points of view for improving our understanding of the thermodynamic stability and the mechanisms that drive folding−unfolding dynamics of proteins.

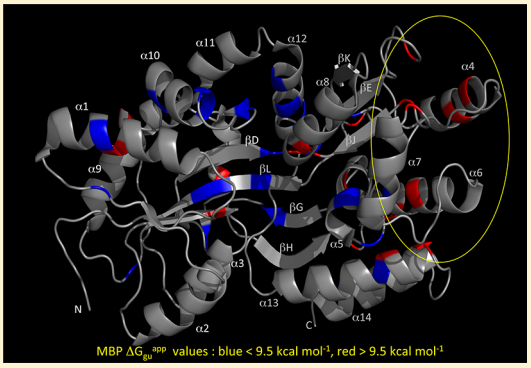

How proteins adopt their specific three-dimensional structure is known as "the protein folding problem" (for a review, see ref 1). It is well-known that proteins unfold and fold repeatedly and that each partially unfolded state, including the fully unfolded state, is significantly populated even under physiological conditions. In favorable cases, the determination of the energy landscape has shown that these partially unfolded states correspond to the major intermediates in the unfolding and refolding pathways, for example, in the case of cytochrome c[2] or Rnase H.[3] NMR spectroscopy is particularly adapted to the characterization of conformational ensembles of partially folded or unfolded states,[4,5] which may contribute to an improved understanding of this question. The NMR hydrogen exchange (HX) method has been used to study protein conformational stability, because it is extremely powerful to identify regions of global or subglobal stability[6−9] and allows the collection of information about the conformational stabilities of individual amino acid residues in a protein structure,[10] which is the key information for elucidating the protein folding problem.

The maltose binding protein (MBP), composed of 370 amino acid residues, is used as a reference protein for characterizing the unfolding process. The structure of MBP was determined by X-ray crystallography (at 2.3 Å[11] and 1.8 Å[12] resolution) and recently by NMR (MBP bound to β cyclodextrin[13−15]). MBP consists of two distinct globular domains (the N-domain: amino acid residues 1−109 and 264−310 and the C-domain: amino acid residues 114−258 and 316−335), connected by three peptide segments (amino acid residues 110−113, 259−263, and 311−315). Each globular domain includes a Rossman fold motif composed of a β-sheet core flanked on both sides by α-helices (Figure 1). The C-terminus does not belong to the globular domains. The binding of maltose to apo-MBP in the interdomain groove is accompanied by a major rotation between the two globular domains around an invariant hinge axis as

Received: March 19, 2012
Revised: October 9, 2012
Published: October 9, 2012

   dx.doi.org/10.1021/bi3003605 | *Biochemistry* 2012, 51, 8919−8930

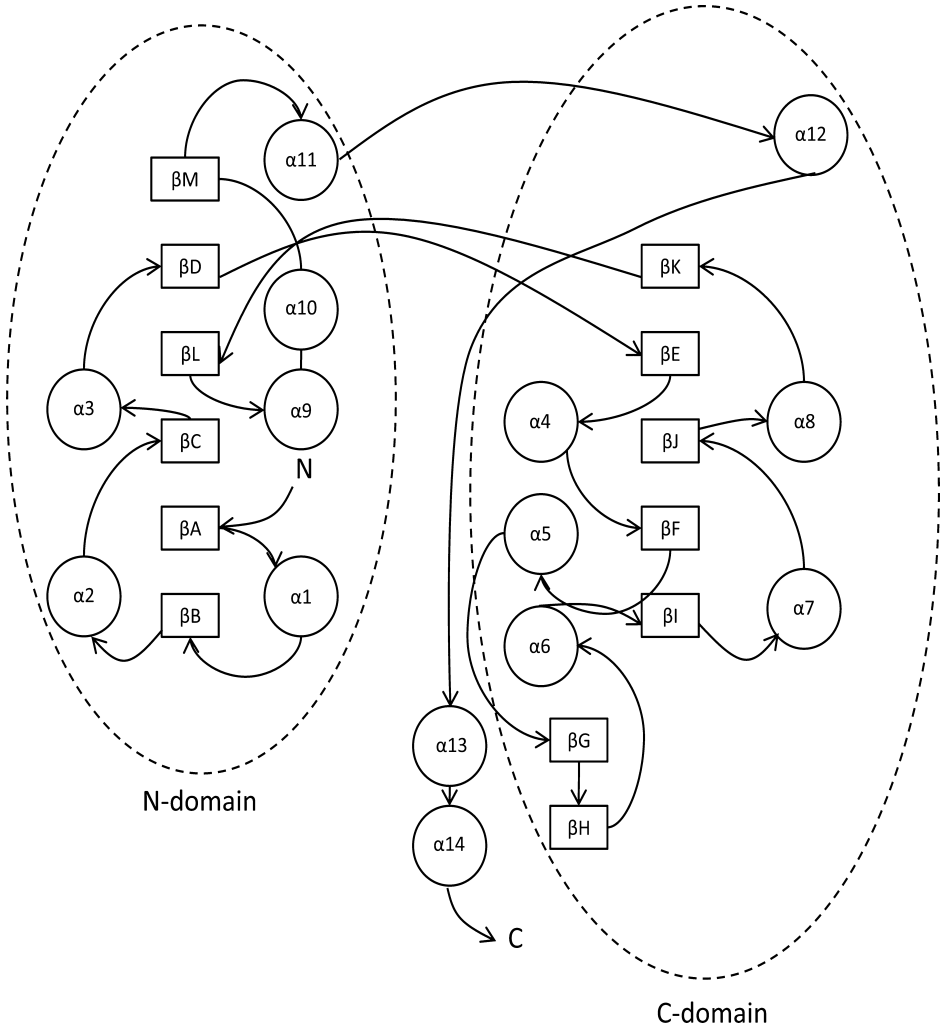

Figure 1. MBP topology.

characterized by various methods (X-ray crystallography,[16] NMR,[17] and molecular dynamics[18]).

Interestingly, MBP is a large protein, among the few exceptions, that unfolds as a single cooperative unit.[19] However, despite intense investigations, information about MBP conformational stability remains difficult to obtain. Thermodynamic parameters of MBP unfolding reactions have been determined. The denaturation of MBP by heating, using guanidine hydrochloride, or at low pH was studied by fluorescence or circular dichroism[19] and compared with urea denaturation.[20] Furthermore, it was shown that maltose increases the cooperativity of MBP unfolding,[21] and recently, its contribution in MBP thermal unfolding was quantified with extrinsic fluorescent dyes.[22] Different MBP destabilized mutants were analyzed to understand the thermodynamic role of particular residues, in the presence of guanidine hydrochloride[23,24] or urea[25] and at different temperatures. Several studies tried to characterize the MBP unfolding pathways. The presence of partially unfolded states of MBP was proposed after the study of its translocation through a biological nanopore (α-hemolysin or aerolysin) by an electric driving force at varying guanidine hydrochloride concentrations. In this study, very long current blockades in nanopores were observed depending strongly on the concentration of the denaturing agent in the vicinity of the denaturation transition.[26,27] Mechanical unfolding of MBP was also investigated. MBP was unfolded using single-molecule force microscopy in combination with cysteine engineering, showing three unfolding intermediates.[28] Finally, by native state proteolysis experiments, the mapping of transient partial unfolding state under native conditions has been proposed.[29]

It thus appears that the determination of the energy landscape of MBP could help in the characterization of its unfolding pathway. We thus produced ^{15}N-labeled MBP to study its stability by NMR combined with fluorescence spectroscopy. NMR HX experiments, conducted under native conditions, allowed us to characterize the protection factors of 180 MBP amino acid residues located all along the sequence. We observed that helix α14 of MBP−βCD has particularly low protection factors. In addition, we conducted HX experiments at subdenaturing guanidine hydrochloride concentrations to differentiate global unfolding events from local fluctuations. The results allowed a partial determination of the energy landscape of MBP−βCD.

MATERIALS AND METHODS

Preparation and Purification of Proteins. The p1H plasmid (generous gift of J.-M. Betton, Institut Pasteur, Paris, France) was used to express MBP in *Escherichia coli* strain BL21 under 50 μg/L ampicillin selection pressure. [^{15}N]MBP labeling was achieved by growing p1H-transformed *E. coli* in a large

dx.doi.org/10.1021/bi3003605 | *Biochemistry* 2012, 51, 8919−8930

volume of M9 medium containing $^{15}NH_4Cl$ (CortecNet, Paris, France) as the sole nitrogen source. To that end, p1H-transformed *E. coli* cultures were grown in series with sequential inoculation respecting the following order: 10 mL of LB medium, 200 mL of M9 medium, and 5 L of M9 $^{15}NH_4Cl$ medium. In the last 5 L culture, when the OD_{600} reached 0.5, overexpression was induced by the addition of 1 mM IPTG. After a 3 h IPTG induction, cells were harvested by centrifugation (4000 *g* for 1 h). Periplasmic MBP was then extracted by osmotic shock.[30,31] Briefly, the pellet was washed twice with 10 mM Tris-HCl (pH 7.2) and resuspended in 250 mL of 30 mM Tris-HCl (pH 7.2), 0.1 mM EDTA, and 20% sucrose. Cells were pelleted by centrifugation (4000 *g* for 1 h). The pellet was osmotically shocked by resuspending the cells in ice-cold water. The suspension was centrifuged (4000 *g* for 1 h), and 20 mM Tris-HCl buffer (pH 7.2) was added to the supernatant. This periplasmic fraction was loaded onto an anion exchange chromatography column for MBP purification (Q-Sepharose, GE Healthcare, Fairfield, CT). Elution was achieved with a linear NaCl gradient (0 to 250 mM) without additions (apo-MBP), with 10 mM maltose (MBP−maltose), or with 10 mM β cyclodextrin (MBP−βCD). Buffer exchange and concentration were achieved by filtration on a 10 kDa cutoff Amicon device (ULTRA-15 10K, Fischer Scientific, Waltham, MA). For NMR experiments, samples were concentrated to 1 mM in 20 mM sodium phosphate buffer (pH 7) using $\varepsilon_{278} = 68750\ M^{-1}\ cm^{-1}$.

Study of Guanidine Hydrochloride-Induced Unfolding by Fluorescence Spectroscopy. Steady state experiments were conducted at 25 °C on a Synergy TM4 thermostated spectrofluorimeter (Bio Tek instruments, Winooski, VT). All samples (apo-MBP, MBP−maltose, and MBP−βCD) were incubated with various concentrations of guanidine hydrochloride for 2 h at 25 °C before measurements were taken. Fluorescence emission spectra were then recorded at 345 nm (excitation at 295 nm), which ensures that the emission is dominated by tryptophan fluorescence.

Theory of Hydrogen Exchange. For structurally protected hydrogens, Linderstrom-Lang proposed a two-state situation:[32,33]

$$\mathrm{NH(closed)} \underset{k_{cl}}{\overset{k_{op}}{\rightleftarrows}} \mathrm{NH(open)} \xrightarrow{k_{rc}} \mathrm{exchanged} \tag{1}$$

with an exchange rate

$$k_{ex} = \frac{k_{rc}k_{op}}{k_{cl} + k_{rc}}$$

Under bimolecular exchange (EX2) conditions where $k_{cl} \gg k_{rc}$ (low pH and temperature), the exchange rate becomes

$$k_{ex} = \frac{k_{rc}k_{op}}{k_{cl}} = k_{rc}K_{op} \tag{2}$$

and the apparent change in Gibbs free energy can be calculated:

$$\Delta G_{HX}^{app} = -RT\ \ln K_{op} = -RT\ \ln\left(\frac{k_{ex}}{k_{rc}}\right) \tag{3}$$

where R is the universal gas constant, T the temperature, and K_{op} the equilibrium constant of unfolding. k_{rc} values were calculated by using SPHERE (http://www.fccc.edu/research/labs/roder/sphere). This software approximates k_{rc} values using hydrogen exchange rates of unfolded oligopeptides.[34,35] We use herein the term "apparent change in Gibbs free energy" like other authors[36] because k_{rc} values are obtained on peptide models, which represents the unique and currently used method for determining random coil rate constants for exchange.[7]

In proteins, the amide hydrogen may undergo HX via global unfolding (gu) or local fluctuations (lf) or both mechanisms. ΔG_{gu}^{app} and ΔG_{lf}^{app} can be obtained according to

$$K_{gu} = \exp\left(\frac{m[\mathrm{GdmCl}] - \Delta G_{gu}^{app}}{RT}\right) \tag{4}$$

$$K_{lf} = \exp\left(\frac{-\Delta G_{lf}^{app}}{RT}\right) \tag{5}$$

$$\Delta G_{HX}^{app} = -RT\ \ln(K_{gu} + K_{lf}) \tag{6}$$

where m represents the denaturant dependence of unfolding.

NMR Spectroscopy. All experiments were performed on 60 μL samples with the MATCH system (Cortecnet, Voisins-Le-Bretonneux, Fr). All NMR spectra were recorded at 37 °C on a Bruker Avance 600 MHz NMR spectrometer equipped with a cryoprobe. Data were acquired and processed using Topspin 2.1 (Bruker, Rheinstetten, Germany).

Chemical Shift Perturbations. Spectra were recorded at 37 °C. To check the sample stability, we compared two HSQC experiments acquired at a 1 week interval. We found that the intensities of HSQC peaks were identical and no supplemental peaks appeared during this delay, which indicates a very good stability of the MBP samples. Spectra were transformed using Topspin 2.0. Chemical shift perturbations were examined at different concentrations of guanidine hydrochloride (0.2, 0.4, 0.6, 0.8, and 1M). Chemical shift differences were calculated using the equation $\Delta\delta = \{(\delta^{1}_{H-1M} - \delta^{1}_{H})^2 + [(\delta^{15}_{N-1M} - \delta^{15}_{N})/6.5]^2\}^{0.5}$ according to Mulder et al.[37] δ^{1}_{H-1M} and δ^{15}_{N-1M} are the chemical shifts observed with MBP−βCD at 1 M guanidine hydrochloride. δ^{1}_{H} and δ^{15}_{N} are the chemical shifts observed with MBP−βCD in phosphate buffer (pH 7). HSQC spectra were recorded with four scans and 256 increments in the ^{15}N indirect dimension. The spectral widths used in both dimensions were 3501 Hz for hydrogen and 3000 Hz for nitrogen.

Hydrogen Exchange Studies and Acquisition of NMR Data. Hydrogen exchange NMR experiments were performed in the absence or presence of guanidine hydrochloride (0.2, 0.3, 0.4, 0.6, and 0.8 M) to stay below the unfolding concentration. The protein samples were lyophilized before being dissolved in D_2O. The samples were then loaded on a pretuned and preshimmed NMR spectrometer, and the HSQC spectra were recorded at different time intervals using the same acquisition parameters as described above.

Amide proton exchange rates, k_{ex}, were determined by fitting the intensity decay of HSQC peaks with a single-exponential curve $I = I_0\ \exp(-k_{ex}t)$ using IGOR Pro (Wavemetrics, OR, USA). Thermodynamic parameters and error bars have been obtained after fitting eqs 4−6 using IGOR Pro. The crystal structure of MBP−βCD at 1.8 Å [Protein Data Bank (PDB) entry 1DMB[12]] was used to visualize and summarize the results. Figures 5 and 8 were generated with PyMOL (The PyMOL Molecular Graphics System, version 1.2r3pre, Schrödinger, LLC, New York, NY).

RESULTS

Evolution of Tryptophan Fluorescence during MBP Unfolding Using Guanidine Hydrochloride. We examined the evolution of the MBP tryptophan fluorescence spectrum depending on the concentration of guanidine hydrochloride in

dx.doi.org/10.1021/bi3003605 | *Biochemistry* 2012, 51, 8919−8930

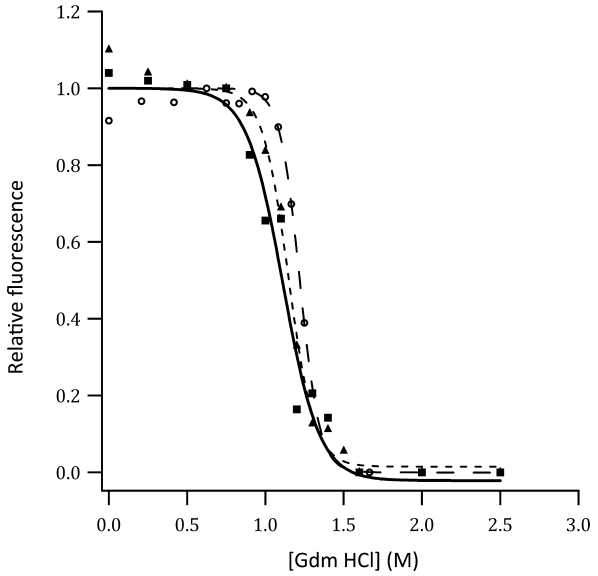

Figure 2. Guanidine hydrochloride denaturation curves of MBP. Evolution of tryptophan fluorescence of MBP (excitation at 295 nm, emission at 345 nm) with guanidine hydrochloride concentration. The experimental curves for apo-MBP (▲), MBP–βCD (■), and MBP–maltose (●) were normalized to 1 in the absence of guanidine hydrochloride by using the relation $f_N = (Y - Y_D)/(Y_N - Y_D)$, where Y_N and Y_D are the fluorescence values of the native and unfolded MBP, respectively. Experiments were conducted at 25 °C in 20 mM phosphate buffer (pH 7).

20 mM phosphate buffer (pH 7) at 25 °C. These spectra reflect changes in the tertiary structure of MBP (Figure 2). We found that MBP unfolds according to a simple two-state process in the presence or absence of ligand, as previously demonstrated.[20,38]

Structural Stability of MBP–βCD Examined via Hydrogen Exchange Experiments. HX experiments were performed under native conditions to calculate protection factors and to obtain thermodynamic parameters at the residue level. As a first step, a two-dimensional HSQC spectrum of MBP–βCD was recorded in phosphate buffer at 37 °C and then compared to that obtained by Gardner et al.[13] This allowed us to assign easily the amide signals of 180 amino acid residues (Figure 3A). We next examined the modifications of this HSQC spectrum with increasing guanidine hydrochloride concentrations (Figure 3B,C) and compared the results to the fluorescence data. We noticed that the global HSQC spectrum of MBP–βCD still shows a large dispersion, which indicates that the protein remains partly in the folded state at 1 M guanidine hydrochloride (Figure 3B), close to the midpoint transition of tryptophan fluorescence (Figure 2). However, some peaks are broadened because of an intermediate exchange (from microsecond to millisecond scale). On the other hand, at 1.5 M guanidine hydrochloride (Figure 3C), the HSQC spectrum becomes characteristic of an unfolded protein, with a narrow dispersion of the peaks. These results are consistent with our fluorescence data.

The study of the thermodynamic parameters involved in the energy landscape, determined by HX experiments, is only possible if the exchange lies in the EX2 regime (bimolecular exchange). Previous calorimetric studies have established the validity of a two-state unfolding model for MBP under the pH conditions used here.[17,19,29] To confirm this proposal, we measured the exchange rates (k_{ex}) of five amino acid residues at different pH values. We observed a linear increase in k_{ex} with pH, which is direct evidence of an EX2 mechanism (Figure S1 of the Supporting Information).

We thus compared the MBP–βCD HSQC spectrum in H_2O/phosphate buffer (pH 7) to that obtained in D_2O/phosphate buffer (pH 7) after 23 min (representing the minimal sample preparation time for HSQC recording). We observed that the amide signals of 57 amino acid residues disappeared in the first D_2O HSQC spectrum because of fast Hydrogen–deuterium (H–D) exchange (Figure S2A,B of the Supporting Information). Consequently, we studied the intensity decay of the 123 remaining amino acid residues by recording a series of HSQC spectra over time. Among them, on the other hand, the intensity of 22 amide peaks stayed very stable over time (see Figure S2C of the Supporting Information). We determined the k_{ex} of the 101 remaining peaks by fitting the data to a single-exponential decay equation (for illustrative examples, see Figure S3 of the Supporting Information), which allowed us to calculate the protection factor (PF = $1/K_{op}$) and ΔG_{HX}^{app} (see eq 3). Results are shown in Figure 4 and Table 1. A log(PF) value of 9 is given to nondecaying peaks, indicating highly protected amino acid residues. A log(PF) value of 3 is given to the 57 rapidly decaying peaks. The uncertainty in the ΔG_{HX}^{app} report is based solely on the measurement of k_{ex} as proposed by Dixon et al.[39]

It can be seen from Figures 4 and 5 that strands βA, βE, and βJ that are located in the core of the globular parts of MBP are particularly protected [with at least two amino acid residues with a log(PF) equal to 9]. A high level of protection is also observed for helices α5, α6, and α9, which are located between the two globular domains [with at least one amino acid residue with a log(PF) of 9]. Interestingly, β-strands βG and βH, located at the edge of the C-domain and close to the C-terminus, show very low protection factors. Furthermore, helix α11 that bridges the N- and C-domains with the C-terminus is less protected than the rest of the two globular parts of MBP. Finally, the last helix of the C-terminus (helix α14) is less protected and is more exposed to solvent exchange. If we observe the MBP structure (Figure 5), it appears that amino acid residues with a high protection factor (red) are in most cases buried in the core of the globular domains, whereas amino acid residues with a low protection factor (blue) are generally exposed on the protein surface.

Structural and Dynamics Perturbations Due to Guanidine Hydrochloride. Amide protons and ^{15}N chemical shifts are sensitive probes of the local environment of a given amino acid residue (see, for example, the work of Wetzel et al.[8] and Mohan et al.[40]) and have a well-established correlation with secondary structure.[41−43] These shifts can thus reflect average changes in hydrogen bond distances and in the ϕ, ψ, and χ torsion angles. The amide ^1H and ^{15}N chemical shifts of the 180 peaks assigned on the HSQC spectrum were measured in H_2O at 37 °C in the absence of guanidine hydrochloride and compared with that observed in the presence of 1 M guanidine hydrochloride. Figure 6 shows the difference in $^1H/^{15}N$ chemical shifts between these two conditions (for superimposition of HSQC spectra, see Figure S4 of the Supporting Information). When we combine these results with the protection factors, three different kinds of behaviors were observed depending on the MBP region. The first group concerns the βE and βJ strands, having high protection factors and small chemical shift perturbations (variations of <0.026 ppm). This suggests that these secondary structures are still not accessible to the solvent even in the presence of 1 M denaturant. The second group (helix α14) is characterized by low protection factors and large

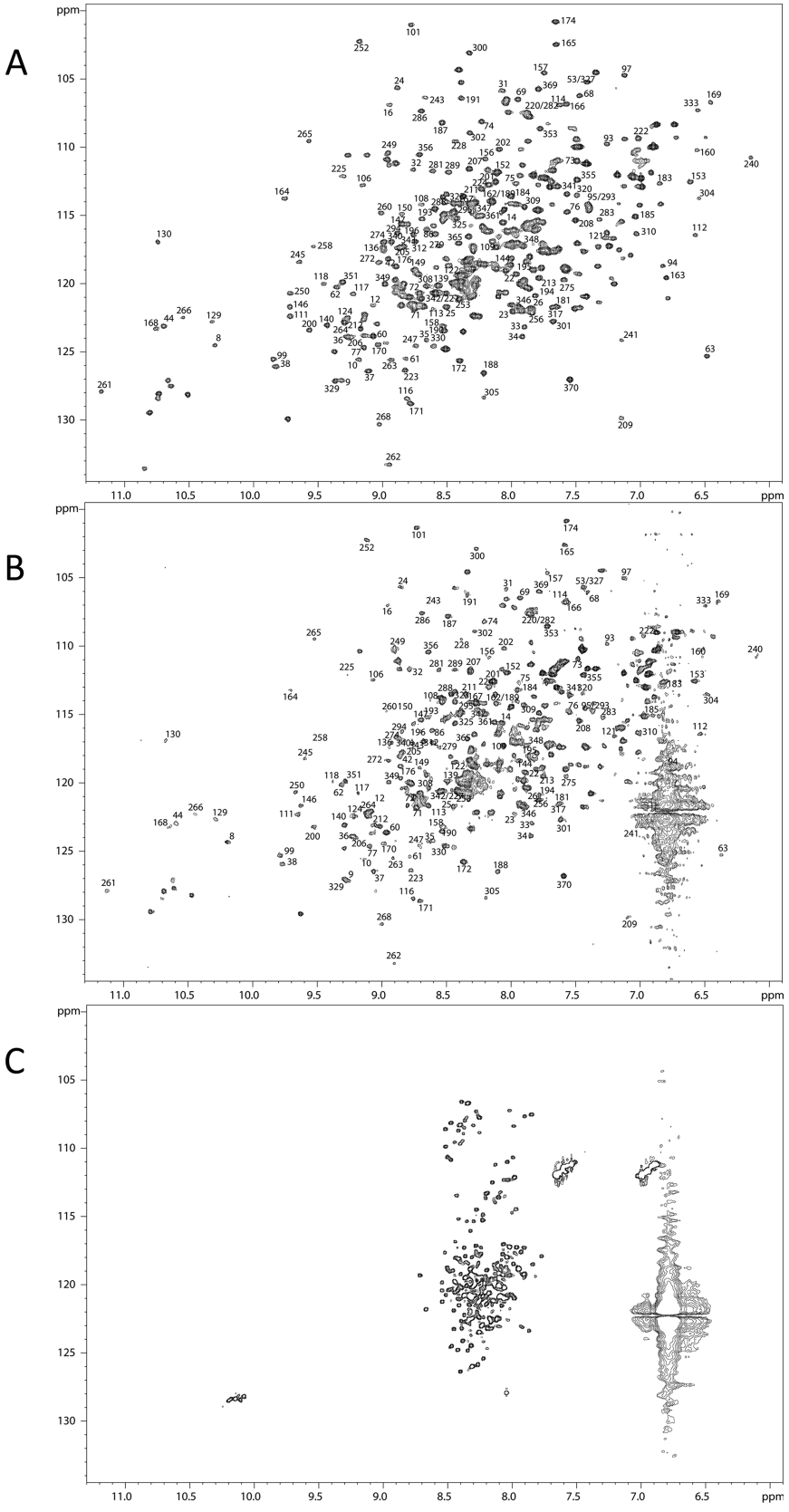

Figure 3. $^{1}H-^{15}N$ HSQC NMR spectra of MBP–βCD in 20 mM phosphate buffer (pH 7) at 37 °C and (A) 0 M, (B) 1 M, and (C) 1.5 M guanidine hydrochloride.

chemical shift perturbations. This suggests environmental perturbations (unfolding or solvent accessibility). The third group is composed of helix α6, which has both a high protection factor and large chemical shift perturbations. This helix, located at the edge of the C-domain, becomes vulnerable to external perturbations in the presence of denaturant but interestingly

dx.doi.org/10.1021/bi3003605 | *Biochemistry* 2012, 51, 8919–8930

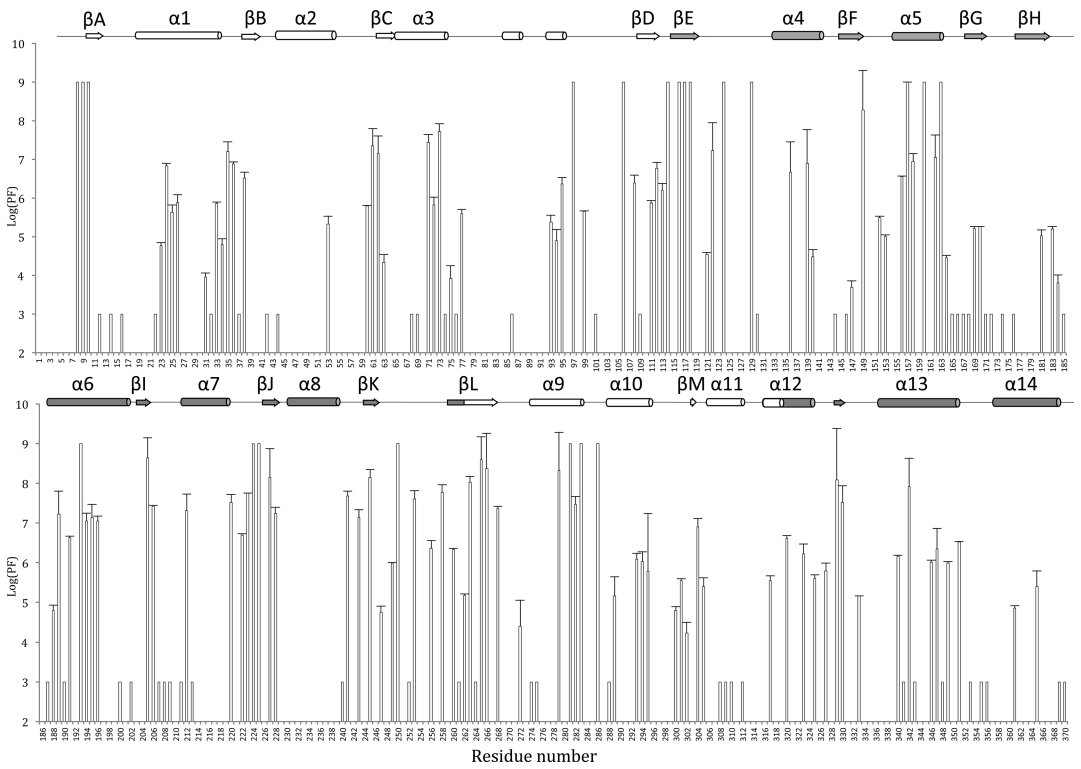

Figure 4. Protection factors for individual amino acid residues of MBP−βCD in 20 mM phosphate buffer (pH 7) at 37 °C (see Table 1). White helices and β-strands belong to the N-domain and gray helices and β-strands to the C-domain.

does not exchange amide protons. Finally, it can be noted that helix α5 implicated in β-cyclodextrin binding (for example E153 or F156) has no important chemical shift perturbations and has intermediate protection factors.

Residue-wise Unfolding Characteristics. Small local fluctuations and larger unfolding events cannot be distinguished in the H−D exchange experiments presented in Figure 4. The apparent change in Gibbs free energy (ΔG_{HX}^{app}) is a combination of both phenomena. It is possible to separate these two contributions using subdenaturing guanidine hydrochloride conditions. The apparent m value is correlated with the maximal increase in accessible surface area upon unfolding.[9,44] In this work, we performed a set of hydrogen exchange experiments in the absence of guanidine hydrochloride and at four different guanidine hydrochloride concentrations (0.2, 0.4, 0.6, and 0.8 M). Under these conditions, 67 amino acid residues could be examined. The contributions of ΔG_{gu}^{app} and ΔG_{lf}^{app} were obtained after fitting the ΔG_{HX}^{app} versus guanidine hydrochloride concentration with eq 4. As illustrative examples, the denaturant dependence of the apparent change in Gibbs free energy for several amide protons exchanges is shown in panels A and B of Figure 7. From this figure and Table 2, we can conclude that both global unfolding and local fluctuations impact MBP amide hydrogen exchange. Many amino acid residues exhibited a near-zero apparent m value (inferior to 0.5 kcal mol^{-1} M^{-1}) in the HX data (for example, amino acid residues 25, 99, 111, ...), indicating that the dynamics are influenced by local events even in the most stable region of proteins, and little surface area is exposed as already noticed for another protein.[2,45,46] Furthermore, the dispersed ΔG_{gu}^{app} values of these amino acid residues (minimum of 6.4 kcal mol^{-1}, maximum of 10.2 kcal mol^{-1}, standard deviation superior to 1 kcal mol^{-1}) suggest that these residues exchange through uncorrelated motion. The apparent m values and the ΔG_{gu}^{app} obtained for individual residues are shown on the native structure of MBP (Figure 8). Amide protons exchanging through the same subglobal unfolding event should share similar values of ΔG_{gu}^{app} and apparent m values. For a protein with partially unfolded states, amino acid residues from an independent unfolding unit will be characterized by the clustering of their ΔG_{gu}^{app} and apparent m values. Figure 8 shows that a correlation could exist between certain ΔG_{gu}^{app} and apparent m values for MBP. As proposed,[47,48] we plotted apparent m values of individual amino acid residues against ΔG_{gu}^{app} (Figure 9). For MBP, it appears that helix α4 and a part of helices α5 and α6 can be clearly grouped into a subdenaturing folding unit, characterizing a high-energy partially folded species. Interestingly, helix α4 has been identified as a small cooperative unfolding unit [amino acid residues D136 and L139 (Figure 7B and Table 2)].

To obtain further information about the stabilities of the different regular secondary structures, we measured hydrogen exchange and protection factors at 310 K at a higher guanidine hydrochloride concentration (1 M). Only the k_{ex} values of residues belonging to the most stable regularly secondary structures were recorded because of strong exchanges.[8] The rates are reported in Table S1 of the Supporting Information and reveal that, in comparison to measurements in the absence of denaturants, exchange is particularly accelerated in helices α4 and α11, and in strands β C−E, G, and L. It is particularly interesting to see that the exchange rates of the amino acid residues from βD implicated in the hinge (amino acid residues 111−113) increase simultaneously, which is consistent with our previous results showing that these amino acid residues have similar ΔG_{gu}^{app} and apparent m values (Table 2). The same remark can be made about the βCD binding site of three amino acid residues (62, 111, and 153). It is noteworthy that strand

dx.doi.org/10.1021/bi3003605 | Biochemistry 2012, 51, 8919−8930

Table 1. Summary of Thermodynamic Parameters (ΔG_{HX}^{app}) Obtained for Individual Residues Using HX

position	residue	ΔG_{HX}^{app} (kcal mol^{-1})	position	residue	ΔG_{HX}^{app} (kcal mol^{-1})	position	residue	ΔG_{HX}^{app} (kcal mol^{-1})	position	residue	ΔG_{HX}^{app} (kcal mol^{-1})
βA	V8	SD		L113	8.75 ± 0.24	α6	F194	9.95 ± 0.37	α10	T286	SD
βA	I9	SD	βE	S114	SD	α6	L195	10.07 ± 0.46	α10	E288	FD
βA	W10	SD	βE	I116	SD	α6	V196	9.95 ± 0.16	α10	G289	7.29 ± 0.67
	N12	FD	βE	Y117	SD	α6	K200	FD	α10	V293	8.59 ± 0.20
	D14	FD	βE	N118	SD	βI	K202	FD	α10	N294	8.51 ± 0.35
α1	G16	FD		L121	6.42 ± 0.06		N205	11.69 ± 0.22	α10	K295	8.16 ± 2.06
α1	E22	FD		L122	10.19 ± 1.01		A206	10.46 ± 0.04		G300	6.76 ± 0.14
α1	V23	6.73 ± 0.10		N124	SD		D207	FD	βM	A301	7.83 ± 0.06
α1	G24	9.64 ± 0.08		W129	SD		T208	FD	βM	V302	5.97 ± 0.37
α1	K25	7.94 ± 0.27		E130	FD	α7	D209	FD	α11	L304	9.74 ± 0.31
α1	K26	8.31 ± 0.13	α4	D136	9.40 ± 1.11	α7	S211	FD	α11	K305	7.62 ± 0.31
α1	T31	5.58 ± 0.02	α4	L139	9.72 ± 1.24	α7	I212	10.46 ± 0.04	α11	E308	FD
α1	G32	FD	α4	K140	6.31 ± 0.12	α7	A213	FD	α11	E309	FD
	I33	8.27 ± 0.06	βF	K144	FD	α7	E214	FD	α11	E310	FD
	L34	6.71 ± 0.21	βF	A146	FD		G220	10.61 ± 0.26	α11	A312	FD
	V35	10.16 ± 0.35	βF	L147	5.21 ± 0.24		T222	9.46 ± 0.06	α12	I317	7.83 ± 0.17
	T36	9.71 ± 0.07		F149	10.65 ± 0.06		A223	6.42 ± 0.06	α12	T320	9.32 ± 0.10
βB	V37	FD		N150	FD	βJ	M224	SD	α12	N323	8.78 ± 0.35
βB	E38	9.17 ± 0.22		Q152	7.75 ± 0.06	βJ	T225	SD	α12	Q325	7.91 ± 0.11
	K42	FD	α5	E153	7.07 ± 0.05	βJ	N227	11.50 ± 1.03		G327	8.17 ± 0.31
α2	E44	FD	α5	F156	9.25 ± 0.01	α8	G228	10.21 ± 0.23		I329	10.12 ± 0.79
α2	T53	7.51 ± 0.20	α5	T157	SD		V240	FD		M330	10.60 ± 0.59
βC	I60	8.18 ± 0.01	α5	W158	9.80 ± 0.58		N241	10.82 ± 0.18		I333	7.28 ± 0.01
βC	F61	10.37 ± 0.63	α5	L160	SD	βK	G243	10.07 ± 1.12	α13	W340	8.69 ± 0.05
βC	W62	10.09 ± 0.64	α5	A162	9.94 ± 0.82	βK	T245	11.42 ± 1.01	α13	T341	FD
βC	A63	6.12 ± 0.46	α5	A163	SD		L247	6.69 ± 0.23	α13	A342	11.16 ± 1.01
α3	G68	FD		D164	6.28 ± 0.09		T249	8.45 ± 0.01	α13	V343	FD
α3	G69	FD		G165	FD		F250	SD	α13	A346	8.49 ± 0.06
α3	A71	10.49 ± 0.30		G166	FD		G252	FD	α13	V347	8.95 ± 0.73
α3	Q72	8.21 ± 0.21	βG	Y167	FD		Q253	10.73 ± 0.06	α13	I348	FD
α3	S73	10.88 ± 0.12	βG	A168	FD		K256	8.97 ± 0.18	α13	N349	8.44 ± 0.06
α3	G74	FD	βG	F169	7.36 ± 0.07	βL	F258	10.96 ± 0.18	α13	A351	9.21 ± 0.01
α3	L75	5.53 ± 0.47	βG	K170	7.42 ± 0.02	βL	G260	8.94 ± 0.02		G353	FD
α3	L76	FD	βG	Y171	FD	βL	V261	FD		Q355	FD
α3	A77	7.89 ± 0.17		E172	FD	βL	L262	7.31 ± 0.05	α14	T356	FD
α3	Q86	FD		G174	FD	βL	S263	11.33 ± 0.20	α14	L361	6.85 ± 0.08
α3	T93	7.89 ± 0.17	βH	Y176	FD	βL	A264	FD	α14	Q365	7.62 ± 0.55
α3	W94	6.90 ± 0.41	βH	V181	7.09 ± 0.21	βL	G265	11.55 ± 0.06	α14	T369	FD
α3	D95	8.99 ± 0.22		V183	7.34 ± 0.09	βL	I266	10.91 ± 0.12		K370	FD
	V97	SD		D184	5.38 ± 0.10		A268	10.40 ± 0.07			
	Y99	7.98 ± 0.03	α6	N185	FD	α9	N272	6.21 ± 0.92			
	G101	FD	α6	G187	FD	α9	E274	FD			
βD	Y106	SD	α6	A188	6.77 ± 0.18	α9	L275	FD			
βD	I108	SD	α6	K189	10.19 ± 0.83	α9	F279	10.79 ± 0.55			
	A109	FD	α6	A190	FD	α9	E281	SD			
βD	E111	8.29 ± 0.08	α6	G191	9.35 ± 0.04	α9	L282	10.54 ± 0.27			
	A112	9.54 ± 0.22	α6	T193	SD	α9	Y283	SD			

βA seems still particularly protected at this high guanidine hydrochloride concentration.

DISCUSSION

Low Structural Stability of the C-Terminus of MBP. We found that the last helix of MBP (helix α14) has low protection factors (Figures 4 and 5). This result confirms the independent behavior of the C-terminus of MBP compared to that of the globular parts of the protein, as previously proposed.[29] Indeed, the C-terminus was already demonstrated as the first to detach from the folded structure using mechanical unfolding.[28] In native state proteolysis experiments, Chang et al. suggested that large parts of helices 13 and 14 correspond to a low-energy state in the energy landscape of MBP.[29] Furthermore, these authors found that the unfolding of these secondary structure elements is uncoupled from the unfolding of the rest of the protein. In agreement with these experimental data, molecular dynamics simulations using unfolding forces on the terminus of MBP demonstrated that helix α14 unfolds first followed by helices α9−α13.[49]

Amino Acid Residues Implicated in the Hinge of MBP Exhibit Similar Thermodynamic Behavior. We can observe that amino acid residues 111−113 and amino acid residues

dx.doi.org/10.1021/bi3003605 | Biochemistry 2012, 51, 8919−8930

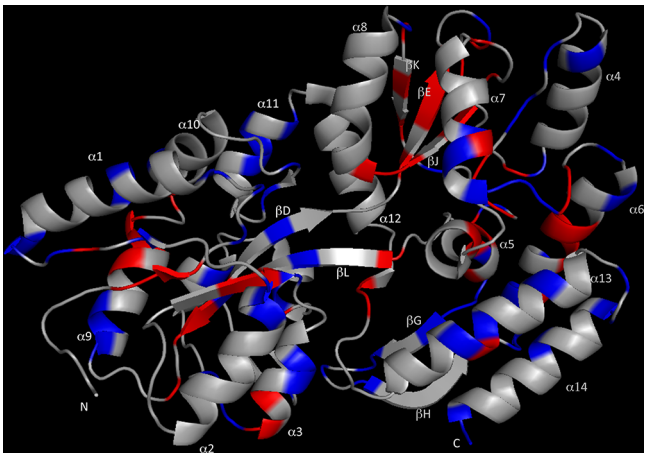

Figure 5. Protection factors are mapped on the crystal structure of the MBP–βCD complex (PDB entry 1DMB[12]). Backbone amide protons that are highly protected [log(PF) superior to 7] are colored red. Backbone amide protons that have low protection factors [log(PF) inferior to 5] are colored blue. The gray portions represent the secondary structure of the C-domain.

260 and 262 (βL strand), which connect the two MBP domains,[11,16] have similar apparent m values (mean value of 0.3 kcal mol^{-1} M^{-1}) and ΔG_{gu}^{app} values (mean value of 8.6 kcal mol^{-1}) (Figure 7A and Table 2). The apparent m value suggests that these amino acid residues unfold through local perturbation. Amino acid residue 263 has a larger ΔG_{gu}^{app} value but is included in the core of the N-domain. These results show that amino acid residues 111–113, 260, and 262 present a similar thermodynamic stability, sharing similar unfolding properties. Interestingly, many studies have demonstrated that the relative orientation of the globular domains of MBP could vary depending on the ligand[50] and that amino acid residues 111–113, 259–263, and 310–315 were acting as a hinge and were implicated in the conformational changes associated with domain closure.[16,51] The third interdomain segment (residues 311–315) is located in a loop. Consequently, exchanges were too fast to be measured, and thermodynamic parameters could not be calculated.

Maltose Binding Site. The amino acid residues implicated in ligand binding for which thermodynamic parameters were obtained (62, 111, 153, and 156) are characterized by an apparent m value inferior to 1, which indicates an unfolding process via local perturbation (Table 2). It is noteworthy that, as demonstrated by Chang et al., the maltose binding site keeps its integrity, even after thermolysin or trypsin cleavage, suggesting a similar and quite high-energy state for these amino acid residues in the MBP energy landscape.[29] A recent study proposes to generate the free energy landscape differences between apo- and holo-MBP based on a molecular simulation approach.[52] Interestingly, it was demonstrated that protein–ligand interaction plays an important role in the mechanical unfolding pathway.[53] A future thermodynamic NMR study of apo-MBP should allow us to illustrate this aspect.

A Partially Folded State, Which Is Weakly Populated under Native Conditions. It has been reported that no populated intermediate state can be detected in bulk experiments during thermal or chemical denaturation.[54] However, we demonstrate here that helix α4 and a part of helices α5 and α6 represent a subdenaturing folding unit under native conditions and that their k_{ex} values increase simultaneously at 1 M guanidine hydrochloride (Table S1 of the Supporting Information). Such partially folded states have already been observed for other proteins.[2,47] These results are compatible with mechanical unfolding studies showing that four structural blocks detached sequentially from

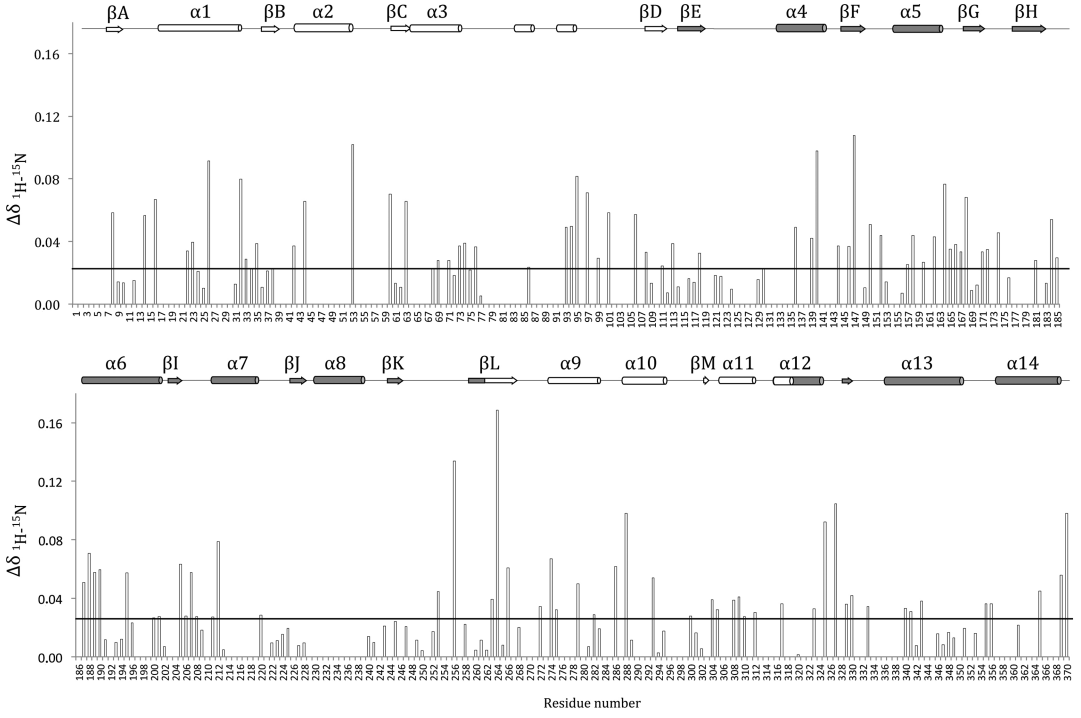

Figure 6. ^{1}H and ^{15}N chemical shift perturbations in the presence of guanidine hydrochloride. Residue specific summed chemical shift changes ($\Delta\delta$) calculated from ΔH_N and ΔN shifts for MBP–βCD in the absence or presence of 1 M guanidine hydrochloride at 37 °C in 20 mM phosphate buffer (pH 7). The horizontal line at 0.026 ppm corresponds to the mean shift (to eliminate important chemical shift variations, we have calculated the average using 85% of the values by excluding the shift variations superior to 0.06 ppm). White helices and β-strands belong to the N-domain and gray helices and β-strands to the C-domain.

dx.doi.org/10.1021/bi3003605 | Biochemistry 2012, 51, 8919–8930

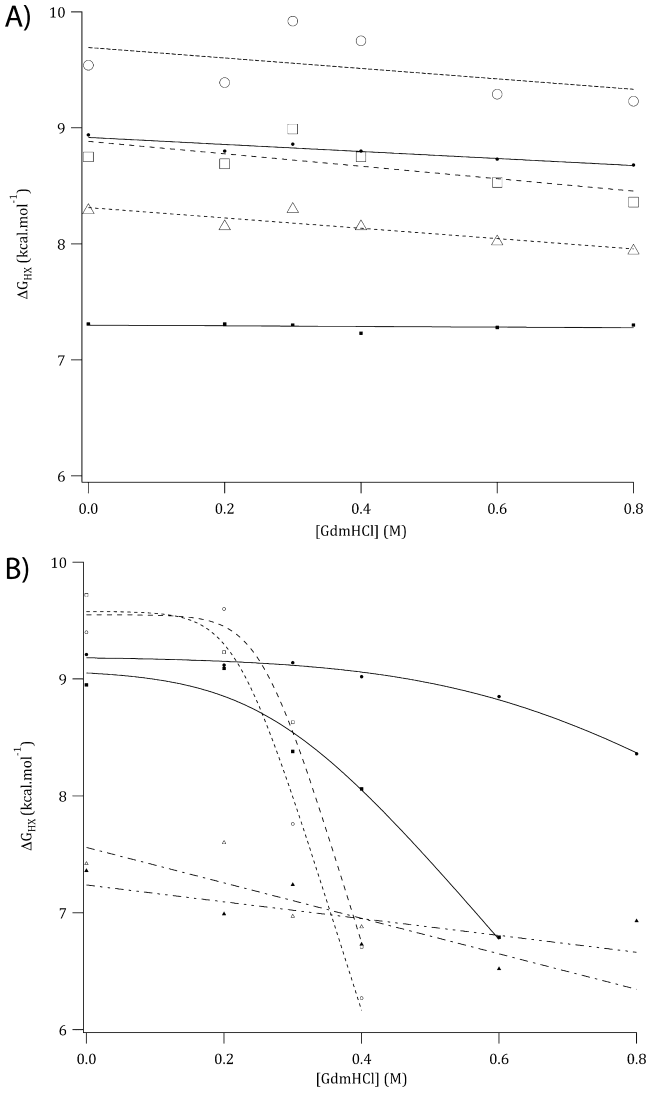

Figure 7. Illustrative examples of the denaturant dependence of the apparent change in Gibbs free energy of hydrogen exchange. The lines represent the fit (eq 6). (A) Empty circles represent data for A112 (belongs to βD, dashed line), empty squares data for L113 (belongs to βD, dashed line), empty triangles data for E111 (belongs to βD, dashed line), filled circles data for G260 (belongs to βL, solid line), and filled squares data for L262 (belongs to βL, solid line). All these amino acid residues belong to the MBP hinge. (B) Empty squares represent data for L139 (belongs to helix α4, dotted line), empty circles data for D136 (belongs to helix α4, dashed line), filled circles data for A351 (belongs to helix α13, solid line), filled squares data for V347 (belongs to helix α13, solid line), filled triangles data for F169 (belongs to sheet βG, dashed and dotted line), and empty triangles data for K170 (belongs to sheet βG, dashed and dotted line).

MBP,[28] helices α4–α6 being part of the fourth block. This fourth block, composed of the whole C-domain, is the last to unfold in the mechanical unfolding experiment. Our NMR results demonstrate the high thermodynamic stability of this part of the C-domain, whereas single-molecule force spectroscopy demonstrates the mechanical stability of the whole C-domain.

Comparison with Single-Nanopore Recording. The results could finally help us to understand long transient conformations that were detected when studying the translocation of protein through single-nanopore recording.[26,55]

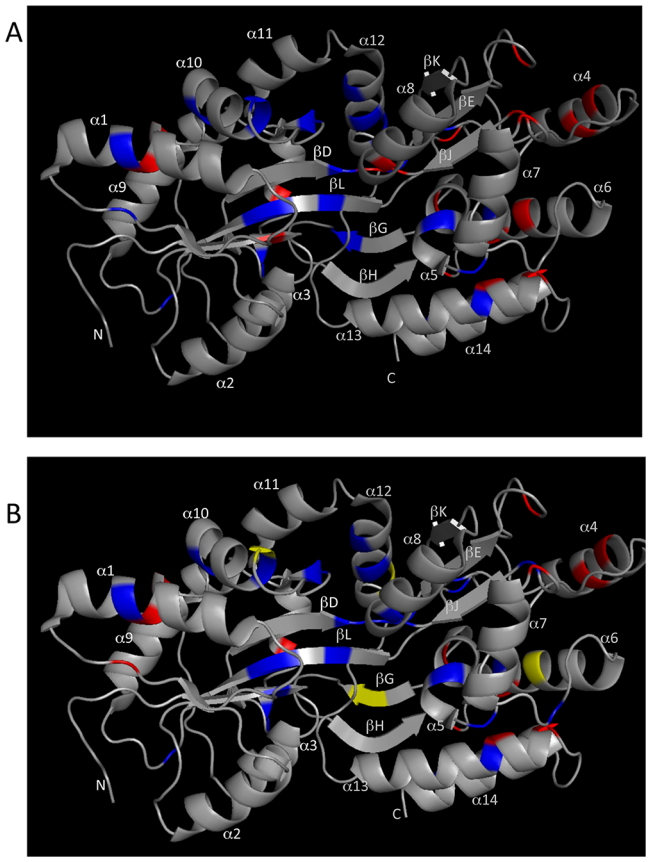

Figure 8. Apparent change in Gibbs free energies of unfolding (ΔG_{gu}^{app}) and apparent m values mapped on the crystal structure of the MBP–βCD complex (PDB entry 1DMB[12]). (A) The range of ΔG_{gu}^{app} values is represented as follows: blue for values inferior to 9.5 kcal mol^{-1} and red for values superior to 9.5 kcal mol^{-1}. (B) The range of apparent m values is represented as follows: blue for values inferior to 1.0 kcal mol^{-1} M^{-1}, yellow for values between 1.0 and 2.0 kcal mol^{-1} M^{-1}, and red for values inferior to 2.0 kcal mol^{-1} M^{-1}.

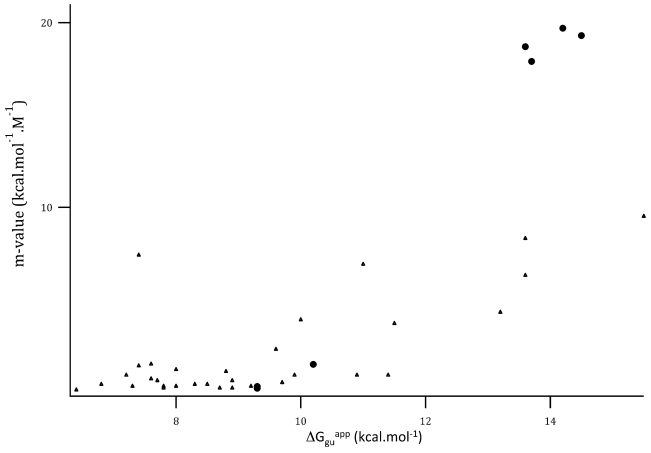

Figure 9. Residue specific hydrogen exchange data of MBP. Apparent m values are plotted vs ΔG_{gu}^{app}. Circles represent data for amino acid residues of helices α4–α6. Data for other amino acid residues from Table 2 are represented with triangles.

In these experiments, long time blockades of the nanopore were observed and interpreted as the penetration of an unfolded segment of the MBP inside the nanopore while a folded part of the protein remained outside of it. Because of the low

dx.doi.org/10.1021/bi3003605 | *Biochemistry* 2012, 51, 8919–8930

Table 2. Summary of the Energetics of Unfolding (apparent m values, ΔG_{lf}^{app}, and ΔG_{gu}^{app}) Obtained for the Individual Amino Acid Residues Using Denaturant-Dependent HX

position	residue	ΔG_{lf}^{app} (kcal mol^{-1})	ΔG_{gu}^{app} (kcal mol^{-1})	m value (kcal mol^{-1} M^{-1})	position	residue	ΔG_{lf}^{app} (kcal mol^{-1})	ΔG_{gu}^{app} (kcal mol^{-1})	m value (kcal mol^{-1} M^{-1})
α1	V23	6.9 ± 0.6			α6	G191		9.3 ± 0.1	0.3 ± 0.1
α1	G24	9.6 ± 0.1	13.2 ± 3.1	4.3 ± 3	α6	L195		10.2 ± 0.3	1.5 ± 0.5
α1	K25		7.8 ± 0.1	0.3 ± 0.1		A206	10.5 ± 0.1		
	I33	8.3 ± 0.1				G220	10.6 ± 0.2	15.5 ± 1.8	9.5 ± 2.5
	L34	6.7 ± 0.1				T222	9.5 ± 0.1		
	V35	10.1 ± 0.4	7.4 ± 1.5	7.4 ± 2.3		A223		10.9 ± 0.1	0.9 ± 0.1
	T36	9.7 ± 0.1			βJ	N227	10.8 ± 0.1		
βB	E38	9.4 ± 0.1			α8	G228		10.2 ± 0.1	0.5 ± 0.2
βC	I60	8.2 ± 0.1				L247		6.8 ± 0.2	0.4 ± 0.3
βC	F61	10.6 ± 0.5				T249	8.5 ± 0.2		
βC	W62		9.9 ± 0.2	0.9 ± 0.4	βL	Q253	10.9 ± 0.1		
α3	T93				βL	G260		8.9 ± 0.1	0.2 ± 0.1
α3	W94				βL	L262		7.3 ± 0.1	0.3 ± 0.1
α3	D95	9.1 ± 0.3	13.6 ± 5	6.3 ± 5		S263		11.4 ± 0.1	0.9 ± 0.2
	Y99		8.0 ± 0.1	0.3 ± 0.1		A268	10.6 ± 0.2		
βD	E111		8.3 ± 0.1	0.4 ± 0.1	α9	N282	10.6 ± 0.1	13.6 ± 0.2	8.3 ± 0.4
	A112		9.7 ± 0.2	0.5 ± 0.4	α10	G289		7.2 ± 0.1	0.9 ± 0.1
	L113		8.7 ± 0.1	0.2 ± 0.1	α10	V293	8.6 ± 0.1		
	L121		6.4 ± 0.1	−0.1 ± 0.9	α10	N294		8.5 ± 0.1	0.4 ± 0.2
	L122		10.0 ± 0.3	3.9 ± 0.6	α10	K295		8.0 ± 0.2	1.2 ± 0.4
α4	D136	9.6 ± 0.4	13.6 ± 1.9	18.7 ± 5.3	βM	A301		7.8 ± 0.1	0.2 ± 0.1
α4	L139	9.5 ± 0.2	14.5 ± 1.7	19.3 ± 4.6	α11	K305	7.6 ± 0.1		
βF	L147	5.8 ± 0.2			α12	I317		7.8 ± 0.1	0.2 ± 0.1
	Q152		7.7 ± 0.9	0.6 ± 0.5	α12	T320		9.2 ± 0.1	0.3 ± 0.2
α5	E153	7.2 ± 0.1			α12	N323		8.8 ± 0.1	1.1 ± 0.3
α5	F156		9.3 ± 0.1	0.2 ± 0.1	α12	Q325	7.8 ± 0.1		
α5	A162	10.1 ± 0.1	13.7 ± 2.4	17.9 ± 6.9		I333	7.2 ± 0.1		
	D164	6.5 ± 0.1				W340	9.0 ± 0.1		
βG	F169		7.4 ± 0.2	1.4 ± 0.4	α13	A346		8.9 ± 0.1	0.6 ± 0.1
βG	K170		7.6 ± 0.3	1.5 ± 0.5	α13	V347	9.1 ± 0.2	11.0 ± 0.7	6.9 ± 1.4
βH	V181	7.3 ± 0.1			α13	A351	9.2 ± 0.1	11.5 ± 0.4	3.7 ± 0.5
	V183	7.5 ± 0.2	9.6 ± 0.5	2.3 ± 0.6	α14	L361	6.9 ± 0.1		
α6	A188	7.1 ± 0.1			α14	Q365		7.6 ± 0.1	0.7 ± 0.2
α6	K189	10.4 ± 2.6	14.2 ± 2.6	19.7 ± 7.7					

thermodynamic stability of the C-terminus of MBP, we can propose that the C-terminal chain of MBP is responsible for channel blockade and that it also contributes to drive the transport of the protein through the nanopore. In the single-nanopore recording experiments, it was also observed that a maximal value of unfolded protein translocation is obtained at 1 M guanidine hydrochloride assimilated to the completely unfolded protein state.[26,55] Interestingly, these NMR results indicate that the tertiary structure of MBP is still present at 1 M guanidine hydrochloride. A first explanation of this apparent difference could be that the peak broadening observed by NMR at 1 M guanidine hydrochloride demonstrates the MBP intermediate conformational exchange (from microseconds to milliseconds). This time scale could correlate with the duration of the blockade observed in the single-nanopore recording. Another hypothesis is that the electrical force applied to the solution in the single-pore recording experiment would be responsible for a decrease in the midpoint of the transition value between the folded and unfolded states. Further investigation is needed to validate one of these hypotheses.

In summary, we have determined the thermodynamic landscape of MBP based on H−D exchange. We have shown that helix α4 and a part of helices α5 and α6 can be clearly grouped into a subdenaturing folding unit, characterizing a weakly populated high-energy partially folded species under native conditions. These results open new perspectives for understanding the ligand influence on MBP thermodynamic stability and, beyond, for understanding the general protein kinetic folding pathway.

■ ASSOCIATED CONTENT

Supporting Information

Comparison of exchange rates at 0 and 1 M guanidine hydrochloride, examples of exchange kinetics, pH dependence of the exchange rates, and superimposition of HSQC spectra at 0 M and 1 M guanidine hydrochloride. This material is available free of charge via the Internet at http://pubs.acs.org.

■ AUTHOR INFORMATION

Corresponding Author

*Present address: Philippe Savarin, Université Paris 13, Sorbonne Paris Cité, CSPBAT, CNRS UMR 7244, 74 rue Marcel Cachin, Bobigny 93017, France. Phone: 33 1 48 38 73 23. Fax: 33 1 49 40 20 36. E-mail: philippe.savarin@univ-paris13.fr.

*Patrick Curmi, Phone: 33 1 69 47 01 87. Fax: 33 1 69 47 02 19 E-mail: pcurmi@univ-evry.fr.

Funding

This work was supported by a grant from Action Thématique Incitative Genopole and ANR Blanche "TRANSFOLDPROT BLANC 08-1_339991".

Notes

The authors declare no competing financial interest.

■ ACKNOWLEDGMENTS

We thank Jean-Michel Betton (Unité de Biochimie Structurale, URA-CNRS 2185, Institut Pasteur, Paris, France) for the generous gift of plasmids and for fruitful discussions. We are particularly grateful to Dr. Vincent Forge (UMR 5090, CEA, Grenoble, France) and Vandana Joshi (UMR 829, INSERM, Evry, France) for critical reading of the manuscript.

■ ABBREVIATIONS

MBP−βCD, maltose binding protein bound to β-cyclodextrin; NMR, nuclear magnetic resonance; HSQC, heteronuclear single-quantum coherence; HX, hydrogen exchange; PF, protection factor.

■ REFERENCES

(1) Dill, K. A., Ozkan, S. B., Shell, M. S., and Weikl, T. R. (2008) The protein folding problem. *Annu. Rev. Biophys. 37*, 289−316.

(2) Bai, Y., Sosnick, T. R., Mayne, L., and Englander, S. W. (1995) Protein folding intermediates: Native-state hydrogen exchange. *Science 269*, 192−197.

(3) Chamberlain, A. K., Handel, T. M., and Marqusee, S. (1996) Detection of rare partially folded molecules in equilibrium with the native conformation of RNaseH. *Nat. Struct. Biol. 3*, 782−787.

(4) Barbar, E. (1999) NMR characterization of partially folded and unfolded conformational ensembles of proteins. *Biopolymers 51*, 191−207.

(5) Korzhnev, D. M., Religa, T. L., Banachewicz, W., Fersht, A. R., and Kay, L. E. (2010) A transient and low-populated protein-folding intermediate at atomic resolution. *Science 329*, 1312−1316.

(6) Dyson, H. J., and Wright, P. E. (1996) Insights into protein folding from NMR. *Annu. Rev. Phys. Chem. 47*, 369−395.

(7) Huyghues-Despointes, B. M., Scholtz, J. M., and Pace, C. N. (1999) Protein conformational stabilities can be determined from hydrogen exchange rates. *Nat. Struct. Biol. 6*, 910−912.

(8) Wetzel, S. K., Ewald, C., Settanni, G., Jurt, S., Pluckthun, A., and Zerbe, O. (2010) Residue-resolved stability of full-consensus ankyrin repeat proteins probed by NMR. *J. Mol. Biol. 402*, 241−258.

(9) Llinas, M., Gillespie, B., Dahlquist, F. W., and Marqusee, S. (1999) The energetics of T4 lysozyme reveal a hierarchy of conformations. *Nat. Struct. Biol. 6*, 1072−1078.

(10) Krishna, M. M., Hoang, L., Lin, Y., and Englander, S. W. (2004) Hydrogen exchange methods to study protein folding. *Methods 34*, 51−64.

(11) Spurlino, J. C., Lu, G. Y., and Quiocho, F. A. (1991) The 2.3-Å resolution structure of the maltose- or maltodextrin-binding protein, a primary receptor of bacterial active transport and chemotaxis. *J. Biol. Chem. 266*, 5202−5219.

(12) Sharff, A. J., Rodseth, L. E., and Quiocho, F. A. (1993) Refined 1.8-Å structure reveals the mode of binding of β-cyclodextrin to the maltodextrin binding protein. *Biochemistry 32*, 10553−10559.

(13) Gardner, K. H., Zhang, X., Gehring, K., and Kay, L. E. (1998) Solution NMR Studies of a 42 kDa *Escherichia coli* Maltose Binding Protein/β-Cyclodextrin Complex: Chemical Shift Assignments and Analysis. *J. Am. Chem. Soc. 120*, 11738−11748.

(14) Mueller, G. A., Choy, W. Y., Yang, D., Forman-Kay, J. D., Venters, R. A., and Kay, L. E. (2000) Global folds of proteins with low densities of NOEs using residual dipolar couplings: Application to the 370-residue maltodextrin-binding protein. *J. Mol. Biol. 300*, 197−212.

(15) Xu, Y., Zheng, Y., Fan, J. S., and Yang, D. (2006) A new strategy for structure determination of large proteins in solution without deuteration. *Nat. Methods 3*, 931−937.

(16) Sharff, A. J., Rodseth, L. E., Spurlino, J. C., and Quiocho, F. A. (1992) Crystallographic evidence of a large ligand-induced hinge-twist motion between the two domains of the maltodextrin binding protein involved in active transport and chemotaxis. *Biochemistry 31*, 10657−10663.

(17) Millet, O., Hudson, R. P., and Kay, L. E. (2003) The energetic cost of domain reorientation in maltose-binding protein as studied by NMR and fluorescence spectroscopy. *Proc. Natl. Acad. Sci. U.S.A. 100*, 12700−12705.

(18) Stockner, T., Vogel, H. J., and Tieleman, D. P. (2005) A salt-bridge motif involved in ligand binding and large-scale domain motions of the maltose-binding protein. *Biophys. J. 89*, 3362−3371.

(19) Ganesh, C., Shah, A. N., Swaminathan, C. P., Surolia, A., and Varadarajan, R. (1997) Thermodynamic characterization of the reversible, two-state unfolding of maltose binding protein, a large two-domain protein. *Biochemistry 36*, 5020−5028.

(20) Sheshadri, S., Lingaraju, G. M., and Varadarajan, R. (1999) Denaturant mediated unfolding of both native and molten globule states of maltose binding protein are accompanied by large ΔCp's. *Protein Sci. 8*, 1689−1695.

(21) Novokhatny, V., and Ingham, K. (1997) Thermodynamics of maltose binding protein unfolding. *Protein Sci. 6*, 141−146.

(22) Layton, C. J., and Hellinga, H. W. (2011) Quantitation of protein-protein interactions by thermal stability shift analysis. *Protein Sci. 8*, 1432−1438.

(23) Betton, J. M., and Hofnung, M. (1996) Folding of a mutant maltose-binding protein of *Escherichia coli* which forms inclusion bodies. *J. Biol. Chem. 271*, 8046−8052.

(24) Raffy, S., Sassoon, N., Hofnung, M., and Betton, J. M. (1998) Tertiary structure-dependence of misfolding substitutions in loops of the maltose-binding protein. *Protein Sci. 7*, 2136−2142.

(25) Prajapati, R. S., Lingaraju, G. M., Bacchawat, K., Surolia, A., and Varadarajan, R. (2003) Thermodynamic effects of replacements of Pro residues in helix interiors of maltose-binding protein. *Proteins 53*, 863−871.

(26) Oukhaled, G., Mathe, J., Biance, A. L., Bacri, L., Betton, J. M., Lairez, D., Pelta, J., and Auvray, L. (2007) Unfolding of proteins and long transient conformations detected by single nanopore recording. *Phys. Rev. Lett. 98*, 158101.

(27) Merstof, C., Cressiot, B., Pastoriza-Gallego, M., Oukhaled, G., Betton, J. M., Auvray, L., and Pelta, J. (2012) Wild type, mutant protein unfolding and phase transition detected by single-nanopore recording. *ACS Chem. Biol. Lett. 7*, 652−658.

(28) Bertz, M., and Rief, M. (2008) Mechanical unfoldons as building blocks of maltose-binding protein. *J. Mol. Biol. 378*, 447−458.

(29) Chang, Y., and Park, C. (2009) Mapping transient partial unfolding by protein engineering and native-state proteolysis. *J. Mol. Biol. 393*, 543−556.

(30) Neu, H. C., and Heppel, L. A. (1965) The release of enzymes from *Escherichia coli* by osmotic shock and during the formation of spheroplasts. *J. Biol. Chem. 240*, 3685−3692.

(31) Kellermann, O. K., and Ferenci, T. (1982) in *Methods in Enzymology Carbohydrate Metabolism: Part E* (Willis, A. W., Ed.) pp 459−463, Academic Press, San Diego.

(32) Linderstrom-Lang, K. (1958) in *Symposium on Protein Structure* (Neuberger, A., Ed.) pp 23−34, Wiley, New York.

(33) Hvidt, A., and Nielsen, S. O. (1966) Hydrogen exchange in proteins. *Adv. Protein Chem. 21*, 287−386.

(34) Bai, Y., Milne, J. S., Mayne, L., and Englander, S. W. (1993) Primary structure effects on peptide group hydrogen exchange. *Proteins 17*, 75−86.

(35) Connelly, G. P., Bai, Y., Jeng, M. F., and Englander, S. W. (1993) Isotope effects in peptide group hydrogen exchange. *Proteins 17*, 87−92.

(36) Itzhaki, L. S., Neira, J. L., and Fersht, A. R. (1997) Hydrogen exchange in chymotrypsin inhibitor 2 probed by denaturants and temperature. *J. Mol. Biol. 270*, 89−98.
(37) Mulder, F. A., Schipper, D., Bott, R., and Boelens, R. (1999) Altered flexibility in the substrate-binding site of related native and engineered high-alkaline *Bacillus* subtilisins. *J. Mol. Biol. 292*, 111−123.
(38) Beena, K., Udgaonkar, J. B., and Varadarajan, R. (2004) Effect of signal peptide on the stability and folding kinetics of maltose binding protein. *Biochemistry 43*, 3608−3619.
(39) Dixon, R. D., Chen, Y., Ding, F., Khare, S. D., Prutzman, K. C., Schaller, M. D., Campbell, S. L., and Dokholyan, N. V. (2004) New insights into FAK signaling and localization based on detection of a FAT domain folding intermediate. *Structure 12*, 2161−2171.
(40) Mohan, P. M., Chakraborty, S., and Hosur, R. V. (2010) Hierarchy of local structural and dynamics perturbations due to subdenaturing urea in the native state ensemble of DLC8 dimer. *Biophys. Chem. 153*, 17−26.
(41) Schwarzinger, S., Kroon, G. J., Foss, T. R., Wright, P. E., and Dyson, H. J. (2000) Random coil chemical shifts in acidic 8 M urea: Implementation of random coil shift data in NMRView. *J. Biomol. NMR 18*, 43−48.
(42) Schwarzinger, S., Kroon, G. J., Foss, T. R., Chung, J., Wright, P. E., and Dyson, H. J. (2001) Sequence-dependent correction of random coil NMR chemical shifts. *J. Am. Chem. Soc. 123*, 2970−2978.
(43) Wishart, D. S., and Sykes, B. D. (1994) Chemical shifts as a tool for structure determination. *Methods Enzymol. 239*, 363−392.
(44) Myers, J. K., Pace, C. N., and Scholtz, J. M. (1995) Denaturant m values and heat capacity changes: Relation to changes in accessible surface areas of protein unfolding. *Protein Sci. 4*, 2138−2148.
(45) Woodward, C. K., and Rosenberg, A. (1971) Studies of hydrogen exchange in proteins. VI. Urea effects on ribonuclease exchange kinetics leading to a general model for hydrogen exchange from folded proteins. *J. Biol. Chem. 246*, 4114−4121.
(46) Englander, S. W., and Englander, J. J. (1978) Hydrogen−tritium exchange. *Methods Enzymol. 49*, 24−39.
(47) Cortajarena, A. L., Mochrie, S. G., and Regan, L. (2008) Mapping the energy landscape of repeat proteins using NMR-detected hydrogen exchange. *J. Mol. Biol. 379*, 617−626.
(48) Wildes, D., Anderson, L. M., Sabogal, A., and Marqusee, S. (2006) Native state energetics of the Src SH2 domain: Evidence for a partially structured state in the denatured ensemble. *Protein Sci. 15*, 1769−1779.
(49) Bechtluft, P., van Leeuwen, R. G., Tyreman, M., Tomkiewicz, D., Nouwen, N., Tepper, H. L., Driessen, A. J., and Tans, S. J. (2007) Direct observation of chaperone-induced changes in a protein folding pathway. *Science 318*, 1458−1461.
(50) Skrynnikov, N. R., Goto, N. K., Yang, D., Choy, W. Y., Tolman, J. R., Mueller, G. A., and Kay, L. E. (2000) Orienting domains in proteins using dipolar couplings measured by liquid-state NMR: Differences in solution and crystal forms of maltodextrin binding protein loaded with β-cyclodextrin. *J. Mol. Biol. 295*, 1265−1273.
(51) Evenas, J., Tugarinov, V., Skrynnikov, N. R., Goto, N. K., Muhandiram, R., and Kay, L. E. (2001) Ligand-induced structural changes to maltodextrin-binding protein as studied by solution NMR spectroscopy. *J. Mol. Biol. 309*, 961−974.
(52) Kondo, H. X., Okimoto, N., Morimoto, G., and Taiji, M. (2011) Free-energy landscapes of protein domain movements upon ligand binding. *J. Phys. Chem. B 115*, 7629−7636.
(53) Aggarwal, V., Kulothungan, S. R., Balamurali, M. M., Saranya, S. R., Varadarajan, R., and Ainavarapu, S. R. (2011) Ligand-modulated Parallel Mechanical Unfolding Pathways of Maltose-binding Proteins. *J. Biol. Chem. 286*, 28056−28065.
(54) Chun, S. Y., Strobel, S., Bassford, P., Jr., and Randall, L. L. (1993) Folding of maltose-binding protein. Evidence for the identity of the rate-determining step in vivo and in vitro. *J. Biol. Chem. 268*, 20855−20862.
(55) Pastoriza-Gallego, M., Rabah, L., Gibrat, G., Thiebot, B., van der Goot, F. G., Auvray, L., Betton, J. M., and Pelta, J. (2011) Dynamics of unfolded protein transport through an aerolysin pore. *J. Am. Chem. Soc. 133*, 2923−2931.